

# Monte Carlo Study of a Luminosity Detector for the International Linear Collider\*

H. Abramowicz<sup>†</sup>, R. Ingber, S. Kananov and A. Levy

*School of Physics and Astronomy, Raymond and Beverly Sackler Faculty of Exact Sciences, Tel Aviv University, Tel-Aviv, ISRAEL*

This paper presents the status of Monte Carlo simulation of one of the luminosity detectors considered for the future  $e^+e^-$  International Linear Collider (ILC). The detector consists of a tungsten/silicon sandwich calorimeter with pad readout. The study was performed for Bhabha scattering events assuming a zero crossing angle for the beams.

## 1. Introduction

The linear collider community has set a goal to achieve a relative precision of  $10^{-4}$  on luminosity measurement. Presently the Forward Calorimetry Collaboration (FCAL) [1] is considering two possible designs for the luminosity detector (LumiCal). Both designs are based on a tungsten/silicon calorimeter. They differ in the readout design, pad or strip. Here we report on studies performed to optimize the performance of the pad readout design.

## 2. Simulation scheme

The Monte Carlo studies, presented in the current note, include simulation of Bhabha scattering, beam-beam interactions, beam spread as well as the full simulation of the LumiCal. For Bhabha scattering events we used BHWIDE [2], a Monte Carlo multi-photon event generator which provides four-momenta of the outgoing electron, positron and photons radiated in the initial and final state. The program CIRCE [3] was used to study the distortion of beam energy spectrum due to beamstrahlung. Two different values of a Gaussian beam spread, 0.05% and 0.5% of the nominal center of mass energy ( $\sqrt{s}$ ), were investigated in the range of beam energy between 50 and 400 GeV. The detector simulation was performed using the BRAHMS [4] package based on the standard GEANT 3.21 simulation program [5]. The performance of LumiCal was studied in three stages,

- with the basic detector design using single electrons/positrons,
- with the basic detector design and a more realistic physics simulation, including simulation of Bhabha scattering events, beamstrahlung and beam spread,
- varying the detector design for optimization purposes.

Fig. 1 shows an example of the center of mass energy spectrum of the  $e^+e^-$  pair originating from Bhabha scattering, including radiative effects, beamstrahlung and a beam spread of  $0.05\%\sqrt{s}$  for nominal 250 GeV beam energies. The main contribution to the tail comes from the initial state radiation in Bhabha scattering.

---

\*This work was partly supported by the Nathan Cummings Chair of Experimental Particle Physics.

<sup>†</sup>also at Max Planck Institute, Munich, Germany, Alexander von Humboldt Research Award.

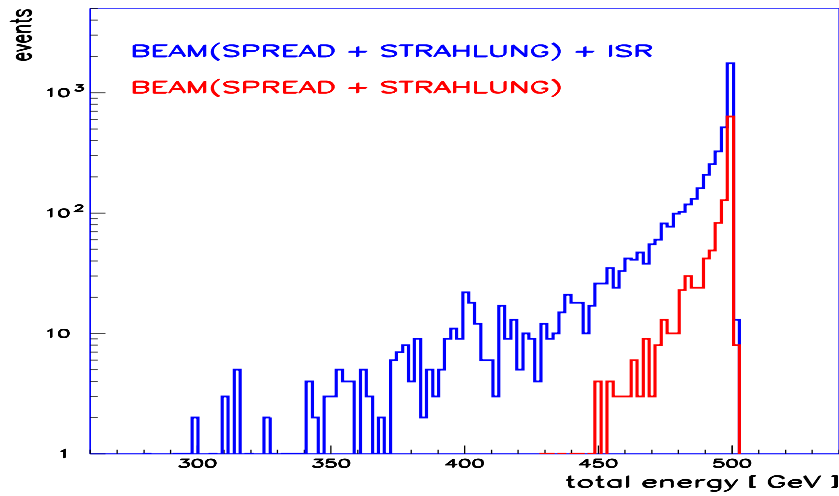


Figure 1: Energy spectrum of the  $e^+e^-$  using BHWIDE and CIRCE at  $\sqrt{s} = 500\text{GeV}$  with a beam spread of  $0.05\%\sqrt{s}$ , with and without initial state radiation, ISR, as described in the figure.

### 3. LumiCal Design

The detector covers polar angles  $\theta$  from 27 to 91 mrad with respect to the beam line. Longitudinally, the detector consists of 30 layers composed each of  $500\ \mu\text{m}$  thick silicon sensors and a tungsten-silicon mixture of 0.34 cm of tungsten and 0.31 cm of silicon and electronics. The detector, with an inner radius of 8 cm and an outer radius of 28 cm, is subdivided radially into 15 cylinders and azimuthally into 24 sectors.

Each layer corresponds to a depth of about one radiation length. The cell transverse size is approximately one *Molière* radius. The total number of cells (electronic channels) is equal to 10,800. Two identical arms, one for the electron side and the second for the positron side, are positioned along the  $z$  axis (beam line), symmetrically with respect to the interaction point (IP), 3.05 m away from the IP.

### 4. Event selection

For luminosity measurement, the geometric acceptance is the most significant event selection rule. The strong  $\theta$  dependence of the Bhabha scattering,  $d\sigma/d\theta \sim 1/\theta^3$ , makes the low angle cut crucial. We used a method, in which only a few layers govern the events selection. In this method the energy deposited in three layers located in the middle of the detector, close to the shower maximum, is divided into energy deposited in the inner edge cylinders,  $E_{out}$  and outside,  $E_{in}$ . The variable,  $p$ , defined as

$$p = \frac{E_{out} - E_{in}}{E_{out} + E_{in}} \quad (1)$$

is then used to estimate the shower containment. Events with  $p > 0$  are rejected as being out of the acceptance region, while events with  $p < 0$  are kept. The behavior of the variable  $p$  as a function of the polar angle of the showering electron is shown in Fig. 2 for three different definitions of  $E_{out}$ , summed over one, two, or three cylinders. A given acceptance cut in  $\theta$  can be translated into an appropriate number of edge cylinders such that a cut on  $p$  will reject the right events without necessity for full reconstruction. The events were preselected using  $p$  only calculated for the electron detector arm. The Bhabha scattering events were further selected by requiring that the showers reconstructed in both arms of the detector be back to back.

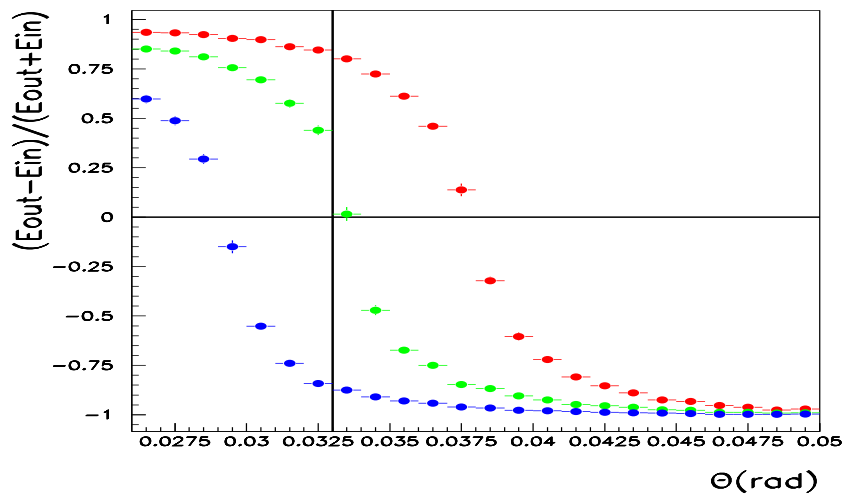


Figure 2: The variable  $(E_{out}-E_{in})/(E_{out}+E_{in})$  as a function of the generated polar angle,  $\theta_{gen}$ , of the showering electrons for  $E_{out}$  summed over one (blue points), two (green points) or three (red points) inner cylinders.

## 5. Position reconstruction

Two approaches were used to reconstruct the position of the shower, with no attempt to reconstruct clusters of energy. The position was determined as the weighted average,

$$\langle x \rangle = \frac{\sum_i x_i W_i}{\sum_i W_i}, \quad (2)$$

where  $x_i$  is the location of the center of the  $i$ -th pad,  $W_i$  is the weight and the sum runs over all pads. The simple, energy weighted average,  $W_i = E_i$ , is known to be biased, with the bias depending on the size of the pads and the impact point of the shower on the pad.

In the second method [6], the weight is assumed to be proportional to the logarithm of the energy deposited, and in addition a cut-off is introduced so that effectively only significant energy deposits contribute,

$$W_i = \max\{0, [const + \ln \frac{E_i}{E_{tot}}]\}, \quad (3)$$

where  $E_{tot} = \sum_i E_i$ . The cut-off,  $const$ , has to be optimized for best resolution. The resolution as a function of cut-off is shown in Fig. 3 for three different incoming energies. The optimal cut-off is found to increase with energy. In parallel, for each cut-off value the bias in reconstructing the position was checked. The point of best resolution turned out to correspond to the least bias.

Just by tuning the cut-off, the polar angle resolution,  $\sigma(\theta)$ , for 250 GeV energy electrons was found to improve by factor three with  $\sigma(\theta) = 0.136 \pm 0.003$  mrad. In addition, the bias was improved by an order of magnitude.

## 6. Detector performance

The polar angle resolution obtained for single particles with the optimal weighting, is shown as a function of the beam energy in Fig. 4, for the various event configurations. Typically, the best resolution is achieved for the single particle MC sample, while for Bhabha scattering with a 0.5% beam spread the resolution is 10% worse.

A small residual bias in the polar angle reconstruction,  $\Delta\theta$ , was observed. For Bhabha scattering with a 0.05% beam spread, the relative value  $\Delta\theta/\theta_{min} = (5.7 \pm 1.3) \cdot 10^{-4}$  is of the same order of magnitude as the required luminosity precision. More statistics is needed to establish, whether this is a genuine effect.

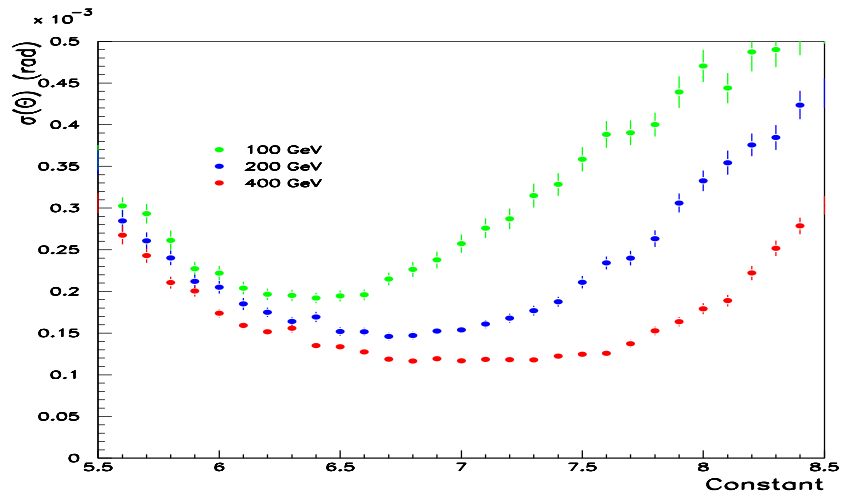


Figure 3: Polar angle resolution,  $\sigma(\theta)$ , as a function of the cut-off value *constants*, for three beam energies, as denoted in the figure.

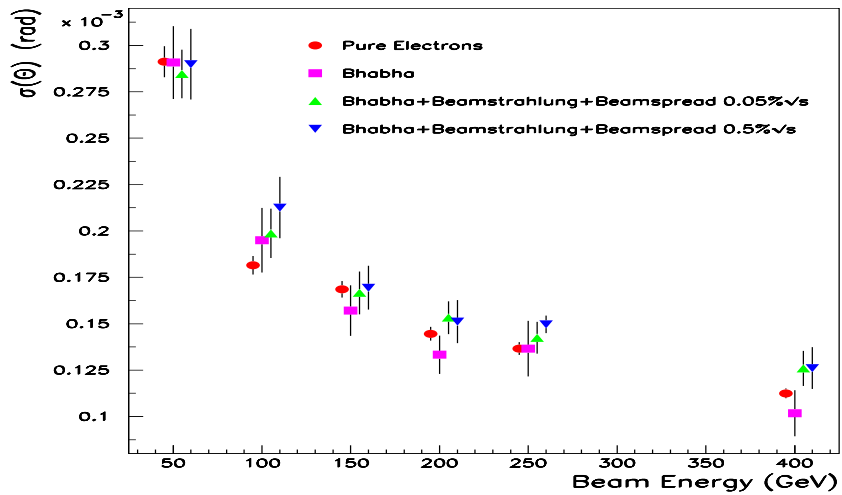


Figure 4: Polar angle resolution,  $\sigma(\theta)$ , as a function of the beam energy for different physics cases, as denoted in the figure.

The energy resolution,  $\Delta E$ , as a function of energy is shown in Fig. 5, again for the various event samples. The resolution follows the expected behavior of  $\Delta E/E = a/\sqrt{E}$ , with  $a$  varying between  $0.24 \pm 0.02$  and  $0.29 \pm 0.03$ . The best resolution is achieved for the sample of Bhabha scattering events with a small beam spread. This is probably due to the requirement that the two showers be back to back, which prevents residual energy leakage.

## 7. Design Optimization

Once the performance of the basic detector design was established, an attempt was made to optimize the depth and the granularity of the calorimeter. For that purpose the calorimeter was assumed to have 50 active layers. A sample of 1000 events was generated for this study.

The angular resolution was studied as a function of the depth and granularity, which was improved by increasing the number of cylinders for the same geometry. The results are shown in Fig. 6. For a given depth of the calorimeter, the resolution is improving with increasing number of readout pads. No improvement is observed beyond a depth of 30 layers. For 30 active layers, increasing the number of cylinders from the 15 of the basic design to 20, leads to an

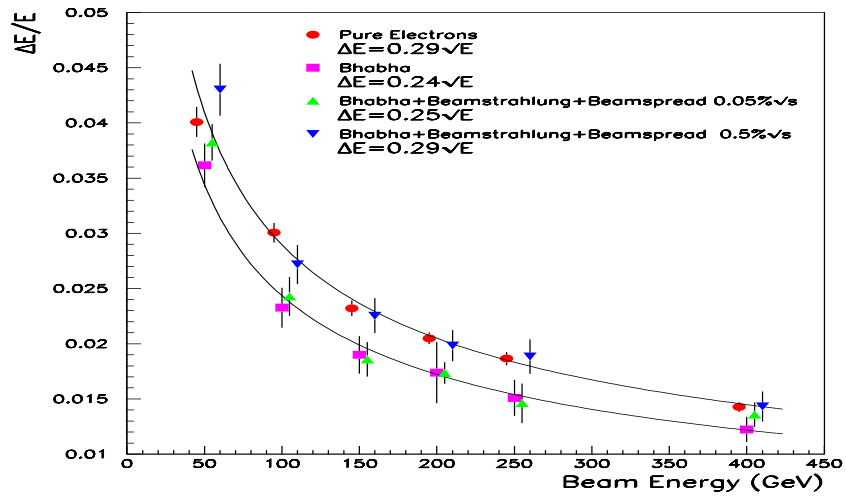


Figure 5: Energy resolution,  $\Delta E$ , as a function of energy for different physics cases, as denoted in the figure.

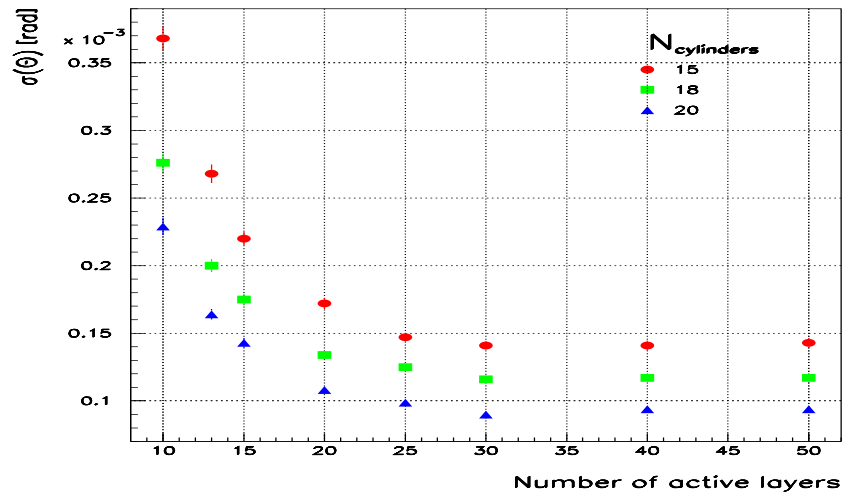


Figure 6: The polar angle resolution,  $\sigma(\theta)$ , as a function of the detector length expressed in terms of active layers, for varying number of cylinders (radial granularity).

angular resolution better than  $10^{-4}$  rad.

The number of sectors was also increased. This improves the resolution of the azimuthal angle, but has no effect on the polar resolution. Increasing the density of the calorimeter would lead to a more compact detector, with less leakage. However the number of pads would have to be increased to match the angular performance of the basic design .

An attempt was made to achieve a better angular resolution by improving the granularity locally, in the layers containing the maximum of the electromagnetic shower. If this is done under the constraint of a fixed total number of readout channels, with 20 cylinders in the inner 15 layers and 10 cylinders in the outer layers, the resolution may be improved by 15%.

## 8. High statistics MC

To achieve sensitivity to systematic effects comparable to the required relative precision on luminosity of  $10^{-4}$ , large statistics MC samples are necessary. This cannot be achieved in a conventional manner, by processing events

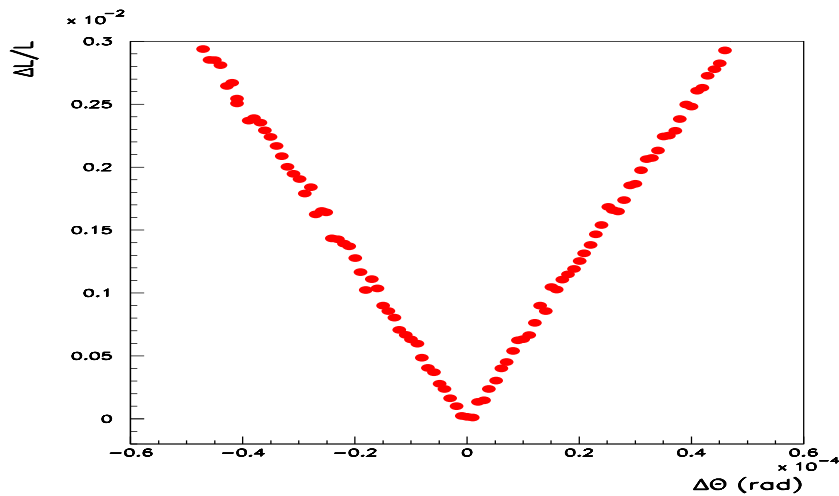


Figure 7: The relative error on the luminosity,  $\Delta L/L$ , as a function of the assumed bias in the polar angle reconstruction,  $\Delta\theta$ .

through a full GEANT simulation. Instead, a fast MC was developed, with smearing effects implemented through parameterization of the performance established on smaller samples. This MC allows detailed studies of various systematic effects, either related to geometry or possible mismatch between MC simulation and detector performance in reality.

The influence of a bias in  $\theta$  reconstruction on the luminosity error, obtained with fast MC simulation, is shown in Fig. 7. Sensitivity to shifts of the order of  $10^{-4}$  are visible. The simulation reproduces well the expected analytical result,  $\Delta L/L = 2\Delta\theta/\theta_{min}$ .

The fast MC was also used to assess whether the presently achieved angular resolution would be sufficient to control the  $\Delta L/L$  with the required precision. Assuming that the Bhabha scattering events are selected by requiring that the two electromagnetic showers be back to back within three times the expected resolution, and assuming a precision of 10% on the resolution itself, would lead to an error on the luminosity,  $\Delta L/L \simeq 5 \cdot 10^{-4}$ . However, if the back to back requirement is relaxed to five times the expected resolution, the projected luminosity error, for the same uncertainty on the resolution, is negligible. Therefore, further studies are needed to understand the required quality for selecting Bhabha candidate events.

## 9. Summary

The luminosity detector at the future linear collider is expected to provide measurements with a precision better than  $10^{-4}$ . In this study, of a tungsten-silicon calorimeter with pad readout, we have concentrated mainly on optimizing the reconstruction algorithms. We have demonstrated that an improvement of a factor of three is possible without changing the granularity. An attempt was also made to optimize the angular resolution by changing the granularity, either by increasing the total number of readout channels or by improving the granularity at the expected shower maximum location while keeping the total number of channels unchanged. A fast MC was developed to study systematic effects with a sensitivity compatible with the required precision.

## References

- [1] H. Abramowicz et al., *Instrumentation of the Very Forward Region of a Linear Collider Detector*, IEEE Transactions of Nuclear Science **51** (2004) 2983.
- [2] S. Jadach, W. Placzek and B. F. L. Ward, *BHWIDE 1.00: O(alpha)YFS Exponentiated Monte Carlo for Bhabha scattering at Wide Angles for LEP/SLC and LEP2*, Phys. Lett. **B390** (1997) 298.

- [3] T. Ohl, *CIRCE version 1.0: Beam spectra for simulating linear collider physics* , hep-ph/9607454.
- [4] T. Behnke, G. Blair, M. Elsing, K. Moenig, V. Morgunov and M. Pohl, *BRAHMS-Version 305, A Monte Carlo for a Detector at 500/800 GeV Linear Collider*, <http://www-zeuthen.desy.de/linear-collider>.
- [5] R. Brun, F. Bruyant, M. Maire A. C. McPherson and P. Zancarini, *GEANT3*, 1984.
- [6] T. C. Awes et al., *A simple method of shower localization and identification in laterally segmented calorimeters*, Nucl. Inst. Meth. **A311** (1992) 130.